Appl. Phys. B (2014) 117:519–526
DOI 10.1007/s00340-014-5863-5

Applied Physics B
Lasers and Optics

Measurements of carbon monoxide mixing ratios in Houston using a compact high-power CW DFB-QCL-based QEPAS sensor

Przemysław Stefański · Rafał Lewicki · Nancy P. Sanchez · Jan Tarka · Robert J. Griffin · Manijeh Razeghi · Frank K. Tittel

Received: 12 March 2014 / Accepted: 19 May 2014 / Published online: 3 June 2014

Abstract Measurements of carbon monoxide (CO) mixing ratios in Houston, Texas, during the period from May 16, 2013 to May 28, 2013 were performed using a sensitive, selective, compact, and portable quartz-enhanced photoacoustic spectroscopy (QEPAS)-based CO sensor employing a high-power continuous wave (CW) distributed feedback quantum cascade laser (DFB-QCL). The minimum detectable CO concentration was 3 ppbv for the strong, interference-free R(6) absorption line at 2,169.2 cm^{-1} and a 5 s data acquisition time. The average CO concentration during the measurement period was 299.1 ± 81.4 ppb with observed minimum and maximum values of 210.5 and 4,307.9 ppb, respectively. A commercially available electrochemical sensor was employed in-line for simultaneous measurements to confirm the response of the CW DFB-QCL-based QEPAS sensor to variations of the CO mixing ratios. Moderate agreement ($R^2 = 0.7$) was found between both sets of CO measurements.

P. Stefański · R. Lewicki · J. Tarka · F. K. Tittel (✉)
Department of Electrical and Computer Engineering, Rice University, 6100 Main Street, Houston, TX 77005, USA
e-mail: fkt@rice.edu

P. Stefański
e-mail: pps2@rice.edu

P. Stefański · J. Tarka
Laser and Fiber Electronics Group, Wroclaw University of Technology, Wybrzeze Wyspianskiego 27, 50-370 Wroclaw, Poland

N. P. Sanchez · R. J. Griffin
Department of Civil and Environmental Engineering, Rice University, 6100 Main Street, Houston, TX 77005, USA

M. Razeghi
Department of Electrical Engineering and Computer Science, Center for Quantum Devices, Northwestern University, 633 Clark Street, Evanston, IL, USA

1 Introduction

Carbon monoxide is a major global pollutant. The main source of its production and emission to the atmosphere is the partial oxidation of carbon-containing compounds associated with combustion processes typically as a result of human activities. Natural sources for atmospheric CO include oxidation reactions of methane and other volatile organic compounds [1–4]. CO, even at low concentration levels, is hazardous to human health and therefore must be accurately and precisely measured. CO should be monitored for healthcare because exposure affects the human respiratory system and can result in dizziness. CO is also an effective biomarker for oxidative stress and anemia [5]. In homes, CO concentrations can be elevated as it is produced by gas and water heaters, stoves and other gasoline powered equipment used in households. Typically, CO levels of 0.5–5 ppm are expected in homes in the absence of high-efficiency heaters and stoves. In spaces where gas stoves/heaters are operated, the CO concentration can increase up to 30 ppm [6].

In this work, a trace gas detection system based on QEPAS [7] was employed to selectively detect and precisely monitor atmospheric CO concentration levels. In a QEPAS-based trace gas sensor, a resonant quartz tuning fork (QTF) is used as the acoustic energy-accumulating element. The QEPAS-based sensor technique benefits from a large quality factor ($Q \sim 8{,}000$ at atmospheric pressure) and resonant frequency (typically $f_{res} = 2^{15} = 32{,}768$ Hz) compared to conventional photoacoustic cells, where typical values for the Q and f_{res} are reported in the range of 40–200 and $f_{res} \sim 1$ k–4 kHz, respectively [7, 8]. In QEPAS, the energy of the modulated light is first absorbed in a gas sample and is then released as heat to create local temperature variations, which subsequently induce acoustic

pressure waves. The interaction between such waves and a QTF leads to deformation of the QTF prongs due to the piezoelectric effect. This deformation results in electric signal generation due to charge separation on electrodes deposited on the QTF prongs [9]. Using a QTF as a piezoelectric transducer is an advantageous approach because an electric signal is created only when anti-symmetric vibrational mode is excited and QTF prongs are moving in opposite directions in the plane of the QTF [10]. Hence, a QEPAS-based sensor is only sensitive to the acoustic waves created between the prongs and is immune to external environmental acoustic noise.

2 Experimental methods

The QEPAS-based sensor used in this study consisted of four distinct components: a 4.61 μm CW DFB-QCL as the QEPAS excitation source, a spatial filter to obtain the best possible DFB-QCL beam shape, an acoustic detection module (ADM) and a control electronics unit (CEU) for 2f detection and data acquisition. The CO measurement system is shown schematically in Fig. 1. A CW high power, room temperature (RT) DFB-QCL grown by molecular beam epitaxy at Northwestern University was placed inside a commercial QCL mounting fixture (Newport, model LDM-4872). The 4.61 μm DFB-QCL emits CW output power levels of up to 1 W when operated at temperatures of ~20 °C. Detailed characterization of this QCL excitation source was reported elsewhere [11, 12]. A spatial filter consisting of two plano-convex CaF_2 lenses and a 300-μm pinhole was inserted after the DFB-QCL in order to minimize non-uniform intensity variations of the QCL beam profile. The purpose of the first 40-mm focal length lens was to focus the beam into a pinhole. The second lens with a 25-mm focal length was used to refocus the diverging beam and to pass it through the microresonator tubes and between the QTF prongs inside the ADM. The inner diameter and length of each microresonator tube were 0.84 and 4.00 mm, respectively. The compact ADM volume allowed for rapid gas exchange. HITRAN-based simulations were performed to determine the optimal line selection and operating pressure conditions for sensitive CO concentration measurements. Water vapor at the 2.5 % level was added to improve the CO relaxation processes and increase the QEPAS signal. Assuming a typical CO mixing ratio of 250 ppb and N_2O atmospheric concentration level of ~320 ppb, an absorbance (base-e) simulation for a spectral region accessible with the 4.61 μm DFB-QCL is depicted in Fig. 2a. The plots depicted in Fig. 2 show that the R(6) absorption line at 2,169.2 cm^{-1} can be detected with the DFB-QCL sensor. The QCL temperature was set to 10 °C in order to maximize its emitted optical power to 280 mW (for $I_{DFB\text{-}QCL} = 750$ mA) after the ADM, since the QEPAS signal intensity scales linearly with power. Multiple experimental scans based on wavelength modulation spectroscopy with a second harmonic detection (2f WMS) technique were performed for different gas mixtures in order to obtain the interference-free R(6) CO absorption line. Figure 2b shows that targeting the R(5) line results in a stronger CO signal but at the same time introduces interference from a neighboring N_2O line.

2.1 Evaluation of sensor performance

A hollow-fiber-based humidification system was employed to add and control water vapor concentration in the sampled mixture in order to improve sensor performance. The addition of 2.5 % of H_2O to the CO containing gas mixture increased the energy transfer for the V-T states of slowly relaxing CO molecules resulting in an ~8 times enhancement of the measured CO QEPAS signal when compared with the result obtained for a dry CO mixture [11, 13–15]. The QEPAS signal amplitude for a calibrated 5 ppm CO: N_2 mixture was investigated for different pressures and modulation depths as shown in Fig. 3a, in order to determine the optimum operating conditions of the reported CO sensor system.

For sensitive atmospheric CO concentration measurements, a 2f-WMS technique was employed when the QCL current was scanned at the rate of 0.2 Hz. The total laser current tuning range required to scan across R(6) CO line was ~60 mA (~0.33 cm^{-1}). The linear response of the sensor system was verified when a certified 5 ppm CO: N_2 mixture was diluted in steps down to 0.25 ppm. The 2f profiles at different CO concentration levels were plotted in Fig. 3b. Linearity of QEPAS sensor response is presented in Fig. 4. The measured data points can be represented by a linear fitting curve with a coefficient of determination equal to $R^2 = 0.99$. A laser frequency locking procedure was employed for the QEPAS-based CO sensor. The line profile was scanned every 5 s. A distinct and smooth 2f profile of CO concentrations in laboratory air was used to implement a control feedback loop that eliminates possible QCL current drift. In this case, a reference cell and photodetector become redundant. For accurate measurements, software control of the QCL operating conditions was implemented to match the 2f line profile of the current scan with the reference one. Atmospheric CO concentration levels were monitored and determined by correlating the 2f-WMS line shape profile for each acquired sample scan with the reference profile taken for a calibrated 5 ppm CO: N_2 mixture that was humidified with 2.5 % of water vapor. Such a profile is shown in Fig. 5. A standard deviation for the minimum detection limit was calculated from the baseline scan when the ADM was filled with humidified pure

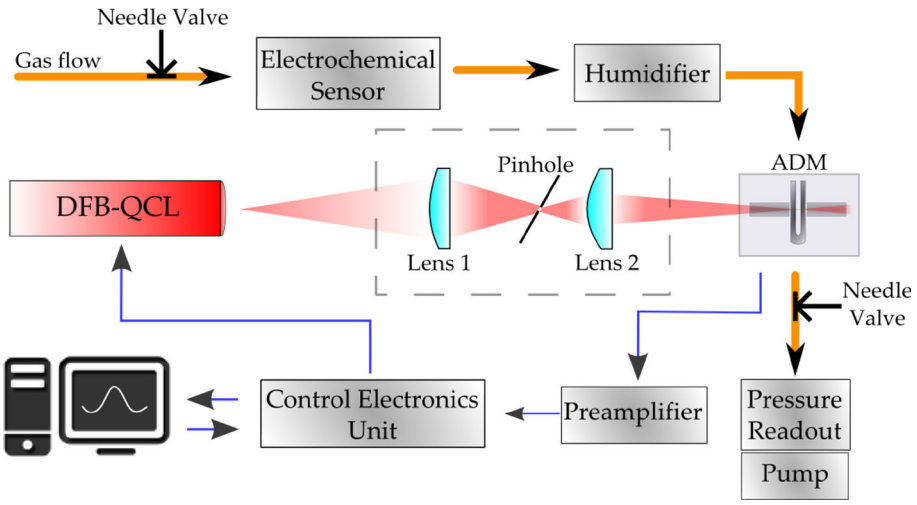

Fig. 1 Schematic diagram of the CW DFB-QCL-based QEPAS CO sensor

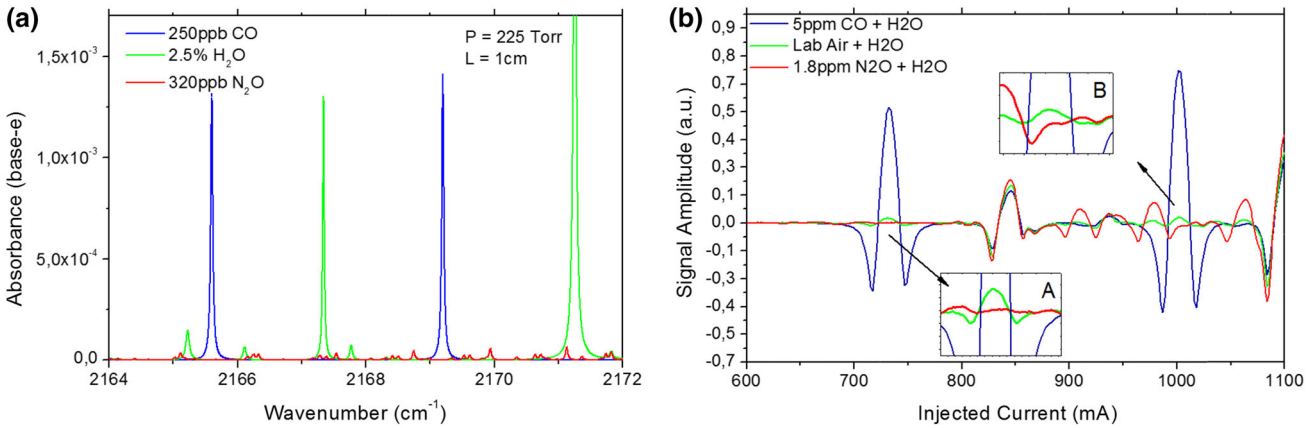

Fig. 2 **a** HITRAN simulation of absorbance for 250 ppb of CO, 2.5 % of H_2O and 320 ppb of N_2O at a pressure of 225 Torr and the optical pathlength of 1 cm **b** 2f scan of entire spectral range at 10 °C. *Inset* A shows the interference-free nature of the R(6) CO absorption line, in comparison with *Inset* B where R(5) CO line is partially overlapping with N_2O line

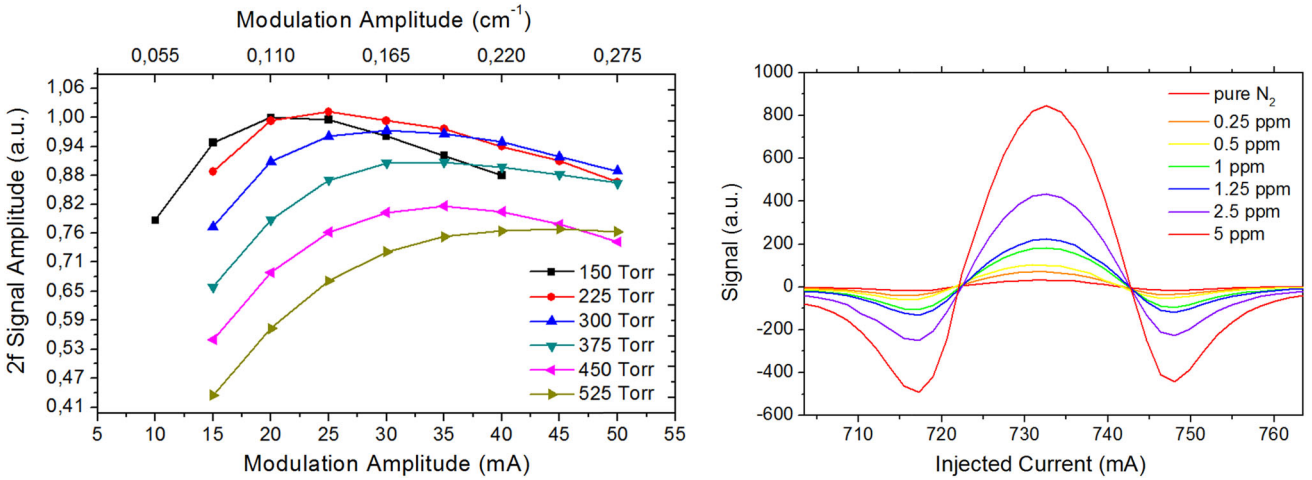

Fig. 3 **a** Normalized 2f amplitude of CO signal as a function of the applied modulation for different operating pressures, **b** 2f profiles for CO mixtures at different concentration levels

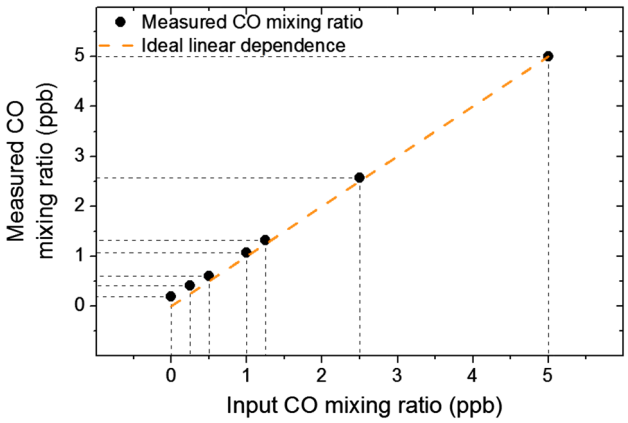

Fig. 4 Linearity of the QEPAS sensor response

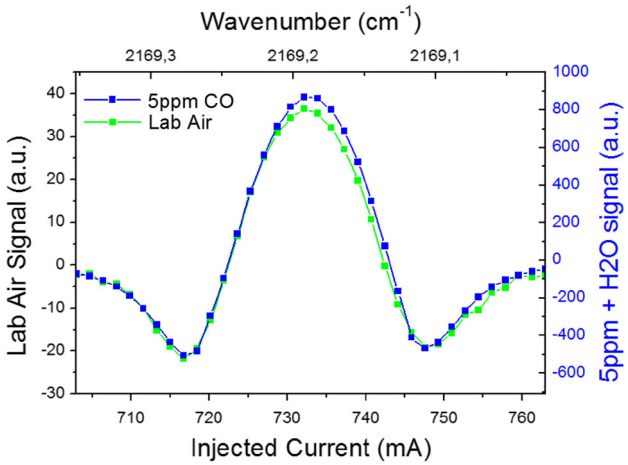

Fig. 5 2f-QEPAS signal for a calibrated 5 ppm mixture of CO:N_2 and 2.5 % water vapor and humidified laboratory air

nitrogen. The optimal modulation depth and operating pressure depend on multiple gas parameters associated with relaxation dynamics [14] and can be measured experimentally. For the reported CO sensor, an optimal pressure of 225 Torr and modulation depth of 25 mA resulted in the best signal-to-noise ratio (SNR) as shown in Fig. 3a. For such a condition, the SNR calculated for the 5 ppm CO: N_2 mixture was ~1,700 and yielded a minimum detectable concentration of 3 ppbv (1σ) for a 5 s data acquisition time. An Allan deviation test was performed to investigate the stability of the CO sensor for long-term measurements. The Allan deviation plot of the CO sensor is shown in Fig. 6. The best result, yielding a measurement resolution of 900 pptv, was achieved with an averaging time of ~100 s, which corresponds to 21 consecutive data points. Typical atmospheric CO mixing ratios in Houston, TX exceed 200 ppbv, a concentration level significantly above the sensor background noise level.

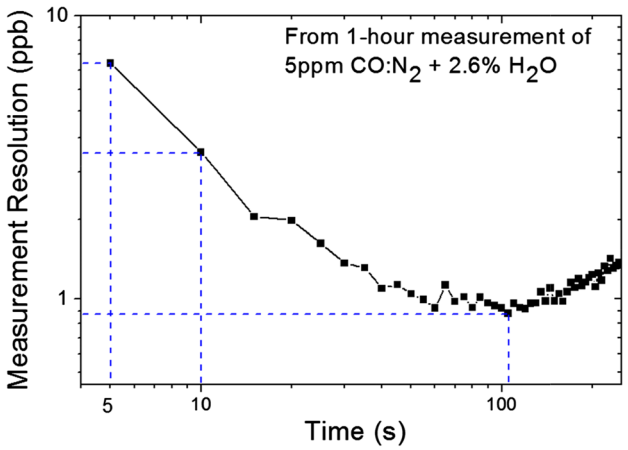

Fig. 6 Allan deviation plot for the CW DFB-QCL-based QEPAS CO sensor system

The footprint of the QEPAS sensor platform was small. All elements essential for sensor operation excluding CEU and water chiller were enclosed in 6″ × 14″ × 8″ plexiglass protective box, which attenuated MIR radiation and ensured eye safety. All optical and mechanical components were attached to a pre-fabricated aluminum baseboard to guarantee mechanical stability and long-term optical alignment. The gas pressure was set to 225 Torr using two needle valves: one at the inlet to restrict gas pressure and the other at the outlet to control gas flow. At low pressures, the gas flow was small enough to guarantee that the analyzed gas was humidified to ~100 % relative humidity regardless of its initial water vapor content. A power meter was installed after the ADM was used to monitor the maximum QCL output power in order to detect any potential misalignment and to perform QEPAS signal normalization. A compact pump was used to perform air sampling for an electrochemical CO sensor (CO B4, Alphasense, UK), installed in-line with the CW DFB-QCL QEPAS-sensor to simultaneously measure CO mixing ratios. Both sensors were evaluated and normalized using a calibrated 5 ppm CO: N_2 mixture. Acquired data allowed for a performance comparison in terms of linearity and response time of both sensors.

2.2 Sampling site

Measurements using a compact DFB-QCL-based sensor were performed on the William Marsh Rice University campus, located 3.5 miles southwest from downtown Houston and within 1.5 miles of two major state highways. The sensor was installed in the Laser Science Group laboratory, and continuous measurements were conducted from May 16 to May 28, 2013, with the gas inlet located outside the laboratory at ground level. Additional data were

obtained from the Texas Commission of Environmental Quality website (http://www.tceq.state.tx.us/), where multiple atmospheric species and parameters are monitored simultaneously, providing hourly averages of temperature, pressure and humidity data. Relevant data were also obtained from a monitoring site located at the University of Houston Moody Tower (UH-MT) [16], which was selected due to its proximity (3.5 miles east) to the Rice University campus.

3 Results and discussion

Temporal variations of CO concentration levels, measured simultaneously with a CW DFB-QCL QEPAS-based CO sensor and a commercial electrochemical CO sensor are presented in Fig. 7. No additional signal smoothing for the scanned QEPAS data (every 5 s) was applied in order to depict the data of high and short concentration peaks shown in Fig. 7. Moderate variability of CO concentration levels at the sampling site was observed. CO concentrations ranged between 210.5 and 4,307.9 ppbv with a mean mixing ratio of 299.1 ± 81.4 ppbv. Statistical analysis of the data indicated that levels between 227.1 and 601.7 ppb (1st and 99th percentile, respectively) were predominant during the period of observation. Some peaks of short duration with concentration exceeding 1 ppmv and a few peaks with levels above 3 ppmv were also detected, suggesting the occurrence of particular traffic-related events that impacted CO levels at the sampling site.

The degree of correlation between the CO mixing ratios measured by the CW DFB-QCL-based QEPAS sensor and the electrochemical instrument is presented in Fig. 8. Moderate agreement was observed between the measurements ($R^2 = 0.7$; slope was calculated using the "Curve fit-linear equation" function in SigmaPlot 12.0), with a high degree of overlapping for mixing ratios below 1 ppmv. Major differences were observed in the concentration range between 1 and 3 ppm, resulting from a difference in response time between the two sensors used in our CO concentration measurements. The main difference between the CW DFB-QCL QEPAS-based sensor and the electrochemical sensor was that the latter integrated the actual mixing ratio over time and therefore was unable to detect a specific peak concentration before it relaxed to typical value. Analysis of the daily variability of the CO concentration (see Fig. 9) showed mean mixing ratios of <300 ppb for most of the monitoring period, with only 2 days exceeding an average of 300 ppb. These high concentration levels were detected on May 17 and May 22, 2013. Low levels of variability in daily CO concentrations were observed during most of the study period with relative standard deviations (RSDs) of <30 %.

CO mixing ratios determined by the DBF-QCL-based QEPAS sensor were consistent with summer time concentrations previously reported for the Houston area, which typically varied between 0.1 and 1 ppm [17, 18]. These previous reports were based on monitoring conducted at the ~70-m high UH-MT sampling site. Comparison of the CO concentrations determined using the CW DBF-QCL QEPAS-based sensor with those measured at the UH-MT site during the sampling period indicated significantly higher mixing ratios at the street level during the monitoring period. Average CO concentrations observed at street level decreased by a factor of 1.7–2.6 as compared to CO measurements performed at the 70-m high UH-MT environmental measurement site (Table 1). The results of this study are consistent with a typical profile previously observed in multiple urban locations impacted by vehicular emissions [19–23] although previous research has not

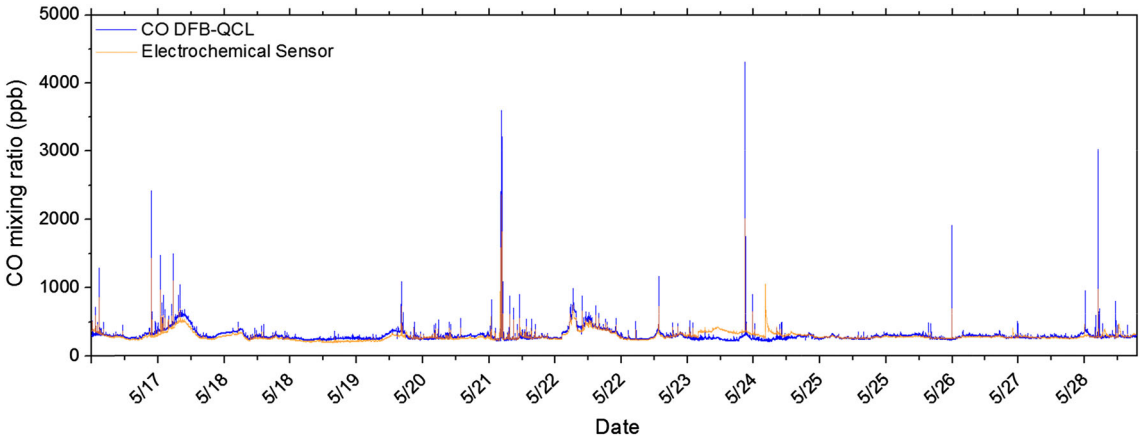

Fig. 7 Time series of CO concentration levels determined using both a CW DBF-QCL QEPAS-based CO sensor and a commercial electrochemical CO sensor (CO B4, Alphasense, UK) during the sampling period from May 16 to May 28, 2013

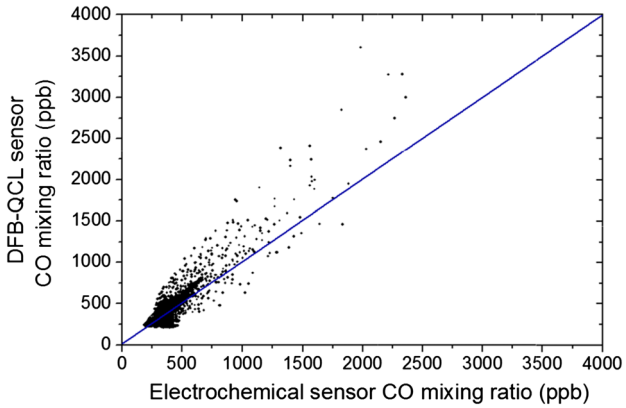

Fig. 8 Correlation between CO mixing ratios determined by the CW DFB-QCL-based QEPAS sensor and the electrochemical sensor during the monitoring period. *Solid line* at 45° indicates equal CO concentration levels ($R^2 = 0.7$, $m = 1.03$)

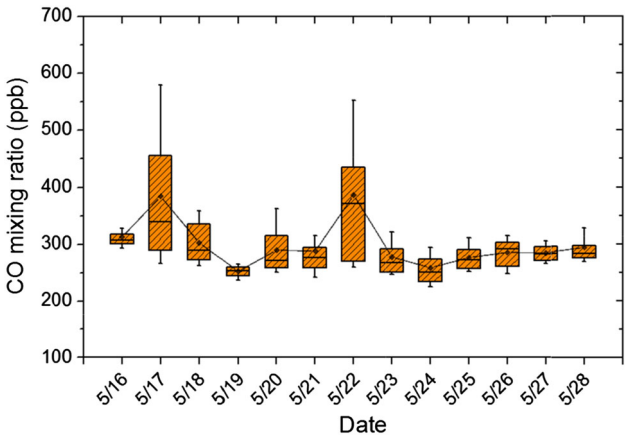

Fig. 9 Daily CO concentration levels determined using the CW DBF-QCL QEPAS-based sensor during the monitoring period from May 16 to May 28, 2013. Bottom whisker, bottom box line, top box line and top whisker indicate the 10th, 25th, 75th and 90th percentile CO concentrations, respectively. *Line inside the boxes* and continuous *solid line* represent the hourly median and mean of the data, respectively

identified a consistent vertical profile for CO concentration measurements [24]. This vertical gradient is characterized by dilution factors between two and five for altitudes ranging between 20 and 60 m. This reduction in the CO concentration has been associated with good mixing and rapid vertical dilution in the atmosphere [19, 21].

The CO mixing ratios measured using the DBF-QCL-based QEPAS sensor during the sampling period did not exceed the National Ambient Air Quality Standards for this molecule, which is 9 ppm (8 h exposure) and 35 ppm (1 h exposure). However, the pronounced differences between street-level and high-altitude (i.e., ~70 m) concentrations suggest that values reported at monitoring stations located at high elevations are not indicative of the exposure of pedestrians to CO. Figure 10 presents the

Table 1 Comparison of CO mixing ratios measured using the CW DBF-QCL-based QEPAS sensor and concentrations reported at UH-MT during the sampling period from May 16 to May 27, 2013

Day of monitoring	Date	Daily mean CO concentration (ppb)		Mean DBF-QCL/Mean UH-MT daily ratio
		DBF-QCL sensor (street level)	UH-MT (~ 70 m)	
1	5/16/13	312.5 ± 33.2	187.0 ± 69.4	1.7
2	5/17/13	383.9 ± 123.8	208.7 ± 90.0	1.8
3	5/18/13	302.9 ± 38.4	134.8 ± 48.7	2.2
4	5/19/13	252.8 ± 45.6	100.0 ± 0	2.5
5	5/20/13	289.8 ± 45.6	126.1 ± 44.9	2.3
6	5/21/13	288.3 ± 123.3	117.4 ± 38.8	2.4
7	5/22/13	385.9 ± 120.0	178.3 ± 79.5	2.1
8	5/23/13	277.6 ± 35.7	126.1 ± 44.9	2.2
9	5/24/13	259.0 ± 68.9	104.3 ± 20.8	2.5
10	5/25/13	277.0 ± 22.8	139.1 ± 50.0	2.0
11	5/26/13	285.9 ± 36.2	147.8 ± 51.1	1.9
12	5/27/13	284.9 ± 17.1	134.8 ± 48.8	2.1
13	5/28/13	293.87 ± 63.2	113.07 ± 34.4	2.6

Midnight to midnight 24-h average CO concentrations are presented for the period between May 17 and May 28, 2013. Mean CO mixing ratio for May 16, 2013 was calculated based on monitoring from 16:00 to 23:59 CST

diurnal profile of the CO mixing ratio during the sampling period as measured by the DFB-QCL-based QEPAS sensor. Average CO levels varied between 277 and 360 ppbv, with lowest concentration levels observed late at night and early in the morning (10:00–03:00 CST). CO increased in the morning and exhibited a maximum concentration during peak traffic conditions between 07:00 and 08:00 CST. A decrease in the CO levels was noticed after 09:00 CST with a continuous reduction during the day, reaching concentrations around 290 ppb after 20:00 CST. A secondary peak of CO concentration (~330 ppb) was observed between 11:00 and 12:00 CST, most likely reflecting an increase in the vehicular activity during this period on the Rice University campus. The high variability associated with the peak shown in Fig. 10 suggests an irregular daily pattern of the traffic activity at this time. Daytime concentrations of CO exhibited higher variability compared with night time measurements during the monitoring period. RSD ranged between 6.7 and 14.3 % and 14.8 and 60.7 % for night and daytime CO levels, respectively.

CO concentration level variations during the monitoring period can be analyzed by comparing weekdays and weekends (Fig. 11). In general, weekday concentrations showed more variability and stronger peaks compared to weekend CO levels (RSD between 4.4 and 25 % and 6.1 and 66 %, respectively). Average weekday concentrations

varied during morning hours increasing from 274 ppb at 01:00 CST and reaching a peak at 07:00–08:00 CST (389 ppb), with a secondary maximum between 11:00 and 12:00 CST (363 ppb). This secondary peak was also observed over the entire monitoring period (Fig. 10) and was not present during weekends, suggesting a typical behavior with recorded weekday traffic activities. A reduction in the CO levels was observed during weekends, with a maximum average concentration of ~ 309 ppbv recorded between 08:00 and 09:00 CST and a subsequent decrease to concentration levels of ~260 ppbv in late evenings. A slight increase in the CO concentration levels was noticed on weekend nights, reaching concentrations of ~290 ppbv.

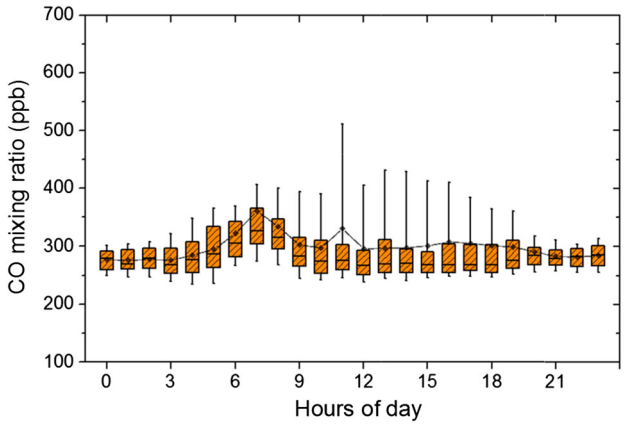

Fig. 10 Diurnal profile of CO mixing ratio during the monitoring period from May 16 to May 28, 2013. *Bottom whisker, bottom box line, top box line* and *top whisker* indicate the 10th, 25th, 75th and 90th percentile concentrations, respectively. *Line inside* the *boxes* and continuous *solid line* represent the hourly median and mean of the data, respectively

4 Conclusions and further development

The recent development of a compact high-power CW DFB-QCL QEPAS-based sensor for CO detection is reported in this paper. For sensitive CO concentration measurements, a strong, interference-free R(6) line located at 2,169.2 cm^{-1} was selected to be the most suitable absorption line within the available CW DFB-QCL spectrum tuning range in terms of absorption coefficient, the DFB-QCL output power, and potential interfering trace gas species. The lack of cross interference from H_2O allowed for an addition of 2.5 % of its vapor to the gas mixture which provided ~8 times enhancement of the QEPAS signal due to an improvement of the intrinsic CO relaxation processes. The CO sensor was operated in a line-scanning mode, where a simplified laser frequency locking procedure was implemented, making a reference cell and detector redundant and thereby resulting in a cost reduction. A high signal-to-noise ratio of ~1,700 for a calibrated 5 ppm CO:N_2 mixture was achieved at an optimal pressure of 225 Torr and modulation depth of 0.14 cm^{-1}, yielding a minimum CO detection limit of 3 ppbv, which is comparable to a previously reported value of 2 ppbv [11], even though the lock-in amplifier time constant used for the measurements was 10 times lower in order to perform much faster absorption line scanning. The reported mid-infrared sensor was found to be stable while averaging the output signal up to ~100 s, providing a measurement resolution of 900 pptv. This value can be further improved by implementing a more sophisticated software laser tuning algorithm that prevents any possible wavelength mismatch between a current and a reference scan.

The sensor was installed in the Laser Science Group laboratory in the Space Science and Technology Building at Rice University in Houston, TX, and used to monitor CO

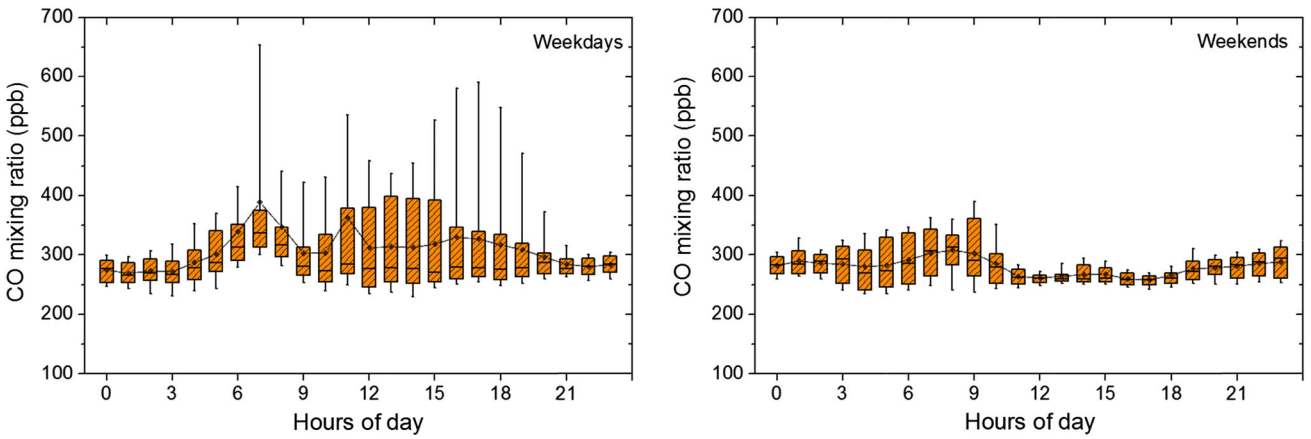

Fig. 11 Weekday and weekend diurnal profile of CO mixing ratios during the monitoring period from May 16 to May 28, 2013. *Bottom whisker, bottom box line, top box line* and *top whisker* indicate the 10th, 25th, 75th and 90th percentile concentrations, respectively. *Line inside* the *boxes* and continuous *solid line* represent the hourly median and mean of the data, respectively

mixing ratios between May 16 and May 28, 2013, with the gas inlet located outside the laboratory on the ground level. Measurement analysis yielded extreme values of 210.5 and 4,307.9 ppbv. The calculated average CO concentration level in the above mentioned period was 299.1 ± 81.4 ppbv. A commercially available electrochemical carbon monoxide sensor was used to verify CW DFB-QCL-based QEPAS system performance and its response. A relatively high ($R^2 = 0.7$) degree of correlation was found between the two sets of measurements, partially reduced by the slower response time of the electrochemical sensor resulting in its inability to detect rapid mixing ratio fluctuations. A complete set of measurement results were consistent with studies reported in the past. The obtained data were used to identify daily and diurnal CO patterns, distinctive for both weekdays and weekends. Additional data provided by Texas Commission of Environmental Quality were also examined. This allowed for a comparison of CO mixing ratios between street level and a higher altitude of ~ 70 m.

Acknowledgments The Rice University group acknowledges financial support from a National Science Foundation (NSF) Grant EEC-0540832 entitled "Mid-Infrared Technologies for Health and the Environment (MIRTHE)", a NSF-ANR award for international collaboration in chemistry "Next generation of Compact Infrared Laser based Sensor for environmental monitoring (NexCILAS)" and the Robert Welch Foundation Grant C-0586.

References

1. M.A.K. Khalil, R.A. Rasmussen, Chemosphere **20**, 227 (1990)
2. J.A. Logan et al., J. Geophys. Res. **86**, 7210 (1981)
3. K.S. Law, Chemosphere Glob. Change Sci. **1**, 263 (1999)
4. C. Zellweger et al., Atmos. Chem. Phys. **9**, 3491 (2009)
5. L.K. Weaver, N. Engl. J. Med. **360**, 1217 (2009)
6. An introduction to indoor air quality (IAQ). Carbon monoxide (CO). http://www.epa.gov/iaq/co.html#Sources, United States Environmental Protection Agency, Web., Cited: 07/03/2013
7. A.A. Kosterev et al., Opt. Lett. **27**, 21 (2002)
8. A. Miklos, P. Hess, Z. Bozoki, Rev. Sci. Instrum. **72**, 1937 (2001)
9. R. Lewicki et al, in *The wonder of nanotechnology: quantum optoelectronic devices and applications*, Chapter. 23, eds by M. Razeghi, L. Esaki, K.V. Klitzing, (SPIE Press, 2013), pp. 597–632
10. N. Petra et al., Appl. Phys. B **94**, 673 (2009)
11. Y. Ma et al., Opt. Express **21**, 11338 (2013)
12. Q.Y. Lu et al., Appl. Phys. Lett. **97**, 04210 (2010)
13. A.A. Kosterev, T.S. Mosely, F.K. Tittel, Appl. Phys. B **85**, 295 (2006)
14. G. Wysocki, A.A. Kosterev, F.K. Tittel, Appl. Phys. B **85**, 301 (2006)
15. A.A. Kosterev, Y.A. Bakhirkin, F.K. Tittel, Appl. Phys. B **80**, 133 (2005)
16. University of Houston Moody Tower (UH-MT), www5.tceq.texas.gov/tamis/index.cfm?fuseaction=report.view_site&CAMS=695, Texas Commision on Environmental Quality, Web, Cited: 7/03/2013
17. W.T. Luke et al., Atmos. Environ. **44**, 4068 (2010)
18. L. Gong et al., Atmos. Chem. Phys. Discuss. **11**, 9721 (2011)
19. S.E. Bauman et al., Atmos. Environ. **16**, 2489 (1982)
20. Y. Qin, S.C. Kot, Atmos. Environ. B Urb. **27**, 3 (1993)
21. M. Väkevä et al., Atmos. Environ. **33**, 1385 (1999)
22. N.M. Zoumakis, Atmos. Environ. **29**, 3719 (1995)
23. A. Bigi, R.M. Harrison, Atmos. Environ. **44**, 2004 (2010)
24. M. Rubio et al., Environ. Monit. Assess. **140**, 161 (2008)